Half-filled one-dimensional extended Hubbard model: Phase diagram and thermodynamics

S. Glocke,[1] A. Klümper,[1] and J. Sirker[2]
[1]*Bergische Universität Wuppertal, Fachbereich Physik, 42097 Wuppertal, Germany*
[2]*Max-Planck-Institute for Solid State Research, Heisenbergstrasse 1, 70569 Stuttgart, Germany*
(Received 6 July 2007; revised manuscript received 12 September 2007; published 24 October 2007)

We study the thermodynamics of the one-dimensional extended Hubbard model at half filling using a density-matrix renormalization group method applied to transfer matrices. We show that the various phase transitions in this system can be detected by measuring usual thermodynamic quantities such as the isothermal compressibility and the uniform magnetic susceptibility. For the isothermal compressibility, we show that universal crossing points exist, which allow us to accurately determine the line where the charge gap vanishes. By studying, in addition, several correlation functions, we confirm the existence of a phase with long-range dimer order (bond order), which has been a matter of debate for several years. According to our calculations, this phase is located in a narrow region between the spin-density and charge-density wave phases up to a tricritical point, which we estimate to be at $U_t=6.7\pm0.2$, $V_t=3.5\pm0.1$. Our results for the phase diagram are in good agreement with the most recent zero-temperature density-matrix renormalization group study; however, they disagree in some important aspects from the most recent Quantum-Monte-Carlo study.

DOI: 10.1103/PhysRevB.76.155121 PACS number(s): 71.10.Fd, 71.10.Pm, 71.10.Hf, 05.70.−a

I. INTRODUCTION

Understanding the effects of competing interactions and the associated quantum phase transitions in models of strongly correlated electron systems is still one of the main issues of modern condensed matter physics. In one dimension, correlation effects are particularly strong and a number of analytical and numerical tools have been developed for this case. This has led to intense work on such systems in the last decades. One of the seminal models in this context is the extended Hubbard model

$$H=-t\sum_{j,\sigma}(c^{\dagger}_{j,\sigma}c_{j+1,\sigma}+\text{H.c.})+U\sum_{j}\left(n_{j,\uparrow}-\frac{1}{2}\right)\left(n_{j,\downarrow}-\frac{1}{2}\right)$$
$$+V\sum_{j}(n_j-1)(n_{j+1}-1)-\frac{h}{2}\sum_{j}(n_{j,\uparrow}-n_{j,\downarrow})-\mu\sum_{j}n_j. \quad (1)$$

Here, $c^{\dagger}_{j,\sigma}$ ($c_{j,\sigma}$) is a creation (annihilation) operator for an electron with spin $\sigma=\uparrow,\downarrow$ at site j, $n_{j,\sigma}=c^{\dagger}_{j,\sigma}c_{j,\sigma}$, and $n_j=n_{j,\uparrow}+n_{j,\downarrow}$. t is the amplitude of a nearest-neighbor hopping, $U\geqslant 0$ an on-site and $V\geqslant 0$ a nearest-neighbor Coulomb repulsion. A possible additional magnetic field is denoted by h, and the chemical potential by μ. Here, we will concentrate on the half-filled case $\mu=0$. In the following, we will only keep the hopping amplitude t where it is necessary for the sake of clarity and set $t=1$ otherwise.

In the strong-coupling limit, $U, V\gg t$, it is easy to see by simple energetic considerations that two different ground states exist: For $U<2V$, the system is an insulator with long-range charge-density wave (CDW) order, whereas for $U>2V$, a state with quasi-long-range spin-density wave (SDW) order forms. The transition between these two phases in the strong-coupling limit is of first order.[1–3] In the weak-coupling limit, $U, V\ll t$, the model can be studied using bosonization and g-ology.[4,5] In this framework, one finds again a phase transition between the SDW and CDW phases at $U=2V$. In the spin sector, this transition is driven by an operator which turns from marginally irrelevant in the SDW phase to marginally relevant in the CDW phase. The spin gap therefore opens up exponentially slowly, and the transition in the spin sector is of Kosterlitz-Thouless (KT) type. In the charge sector, on the other hand, there is a relevant operator in both phases leading to a charge gap. The amplitude of this operator vanishes only at the transition line $U=2V$, so that the charge gap disappears.[4] The transition in the charge sector is therefore of second order. Already from the strong- and weak-coupling approaches, it is clear that a point (U_t, V_t) in the intermediate coupling regime must exist where the order of the phase transition changes.

In the last few years, the extended Hubbard model has attracted renewed attention because it has been suggested that the phase diagram obtained by the weak-coupling g-ology approach and strong-coupling perturbation theory might not be complete. Nakamura pointed out first that there is no symmetry requiring the lines in U, V-parameter space, where the marginal operator in the spin sector changes sign and where the relevant operator in the charge sector vanishes, to coincide.[4,6] The coupling constants for these two operators do coincide in the standard g-ology approach, where they are calculated to first order in the interaction parameters. However, they might differ once higher order corrections are taken into account. This opens up the possibility for an intermediate phase. By extracting the scaling dimensions related to the critical exponents of certain correlation functions from finite-size energy spectra, Nakamura indeed found a phase with long-range dimer order in a small region between the SDW and CDW phases. This phase is often called a bond-order wave (BOW) state. The existence of such a phase around $U=2V$ in the weak-coupling regime was supported by quantum Monte Carlo (QMC) calculations[7,8] as well as by a g-ology approach where the coupling constants have been calculated beyond leading order.[9] However, in a first density-matrix renormalization group (DMRG) calculation,[10] such a phase was only found

above the tricritical point (U_t, V_t) and only directly at the first order transition line. A later DMRG calculation,[11] on the other hand, qualitatively confirms again the phase diagram as proposed by Nakamura. Further evidence for the existence of a BOW phase in the weak-coupling regime was also provided by a functional renormalization group analysis.[12]

Although the most recent DMRG[11] and the most recent QMC study[8] agree that a BOW phase of finite extent does exist, they disagree about the shape of this phase. Whereas in the phase diagram of Ref. 11 the BOW phase ends at the tricritical point, it extends beyond this point to larger values of U, V in the phase diagram of Ref. 8. The question whether the tricritical point also marks the end of the BOW phase or is located on the BOW-CDW boundary therefore remains an open issue.

In this work, we will investigate the half-filled one-dimensional extended Hubbard model using a density-matrix renormalization algorithm applied to transfer matrices (TMRG). This numerical method allows it to calculate thermodynamic properties of the model in the thermodynamic limit. We will provide further evidence for the correctness of the phase diagram as first proposed by Nakamura and give an estimate for the tricritical point (U_t, V_t). In particular, we will argue based on our numerical results that the BOW phase ends at the tricritical point and does not extend to larger values of U, V, in contrast to the findings in Ref. 8. In the process, we will develop and discuss criteria to identify the different phases and transition lines by considering usual thermodynamic quantities such as the uniform magnetic susceptibility, the isothermal compressibility (charge susceptibility), and the specific heat.

Our paper is organized as follows. In Sec. II, we briefly introduce the TMRG algorithm and compare results for the Hubbard model ($V=0$) with exact results obtained by the Bethe ansatz. In Sec. III, we then present results for a variety of thermodynamic quantities which allow us to determine the phase diagram of the extended Hubbard model at half filling. The last section is devoted to our conclusions.

II. TRANSFER-MATRIX RENORMALIZATION GROUP ALGORITHM AND THE HUBBARD MODEL

The density-matrix renormalization group applied to transfer matrices (TMRG) has been explained in detail in Refs. 13–15. Here, we only want to briefly discuss the most important aspects. The TMRG algorithm is based on a mapping of a one-dimensional quantum system to a two-dimensional classical one by means of a Trotter-Suzuki decomposition. In the classical model, one direction is spatial whereas the other corresponds to the inverse temperature. For the classical system, a so-called quantum transfer matrix (QTM) is defined which evolves along the spatial direction. At any nonzero temperature, the QTM has the crucial property that its largest eigenvalue Λ_0 is separated from the other eigenvalues by a finite gap. The partition function of the system in the thermodynamic limit is therefore determined by Λ_0 only, allowing it to perform this limit exactly. The Trotter-Suzuki decomposition is discrete so that the transfer matrix has a finite number of sites or local Boltzmann weights M. The temperature is given by $T \sim (\epsilon M)^{-1}$, where ϵ is the discretization parameter used in the Trotter-Suzuki decomposition. The algorithm starts at some high-temperature value where M is so small that the QTM can be diagonalized exactly. Using a standard infinite-size DMRG algorithm, sites are then added to the QTM leading to a successive lowering of the temperature. A source for a systematic error in these calculations is the finite discretization parameter ϵ. However, this only leads to errors of order ϵ^2 in all thermodynamic quantities considered in the following. We will choose $\epsilon=0.025$ or 0.05 so that this systematic error will only be of order $10^{-3}-10^{-4}$. Another error is introduced by the truncation of the Hilbert space. This error will grow with decreasing temperature and will finally make the calculations unreliable. Down to which temperature the DMRG algorithm works will depend on the maximum number of states N kept in the truncated Hilbert space basis. The truncation error is difficult to estimate. We therefore start by comparing our TMRG results for the Hubbard model ($V=0$) with exact results obtained by the Bethe ansatz.[16] Within the TMRG algorithm, nothing changes fundamentally when we introduce the nearest-neighbor Coulomb repulsion V so that we expect a similar accuracy in this case.

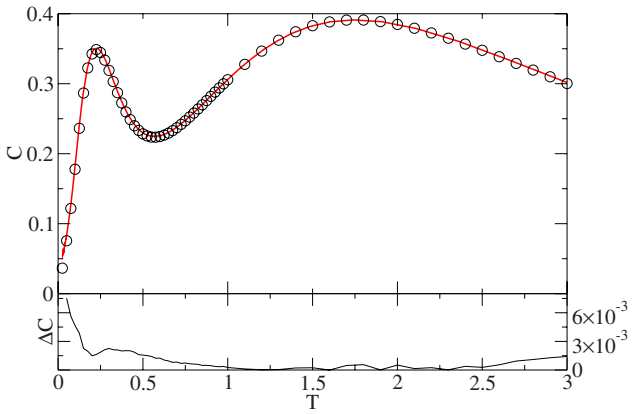

FIG. 1. (Color online) TMRG data for the specific heat C of the Hubbard model at $U=8$ with $N=200$ states kept (red solid line) compared to Bethe ansatz data (circles) as a function of temperature T. The lower graph shows the error ΔC of the TMRG calculation.

As an example, we consider the case $U=8$. Results with a similar accuracy are also obtained for other U. Using the TMRG method, the free energy per site is given by

$$f = -T \ln \Lambda_0. \tag{2}$$

The specific heat is then obtained by $C=-T\partial^2 f/\partial T^2$ and is shown in Fig. 1. It is also easy to calculate the expectation values of local operators with the TMRG algorithm. To obtain the magnetic susceptibility χ_s, the expectation value $m \equiv \langle S^z \rangle = \langle n_\uparrow - n_\downarrow \rangle /2$ is calculated in the presence of a small magnetic field $\delta h \sim 10^{-2}$. The susceptibility is then given by $\chi_s = m/\delta h$ and shown in comparison to the exact result in Fig. 2. Similarly, the isothermal compressibility (charge susceptibility) χ_c is obtained by applying a small chemical potential $\delta\mu$ and is shown in Fig. 3. For the spin and charge susceptibilities χ_s and χ_c, the error does not exceed 5×10^{-4} down

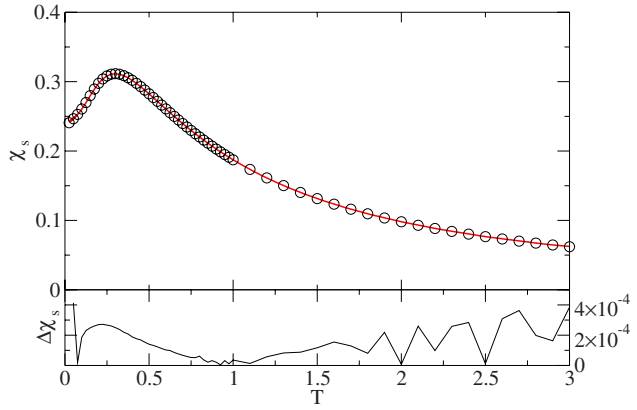

FIG. 2. (Color online) Same as Fig. 1 for the magnetic susceptibility χ_s.

to temperatures $T \approx 0.05$. For the specific heat C, the errors are an order of magnitude larger because a second numerical derivative has to be calculated.

III. PHASE DIAGRAM OF THE EXTENDED HUBBARD MODEL AT HALF FILLING

To investigate the phase diagram, we will consider a number of different thermodynamic quantities such as magnetic susceptibilities, compressibilities, specific heats, and expectation values of local operators. Furthermore, we will study the behavior of correlation lengths which can be obtained within the TMRG method by calculating next-leading eigenvalues of the QTM.[13,15] Depending on the required accuracy and the temperature regime we want to access, the basis for the truncated Hilbert space will consist of $N=200-400$ states.

We start with the strong-coupling limit where the two existing phases and the first order phase transition between these phases are well understood. We then derive an estimate for the tricritical point where the first order line ends. Next, we discuss the considerably more complicated weak-coupling regime and present the phase diagram as obtained by TMRG. Finally, we will address the controversial question whether or not the BOW phase ends at the tricritical point. Throughout, we will discuss how far one can identify the different phases and phase transitions by studying only easily measurable thermodynamic quantities such as the specific heat, magnetic susceptibility, and compressibility.

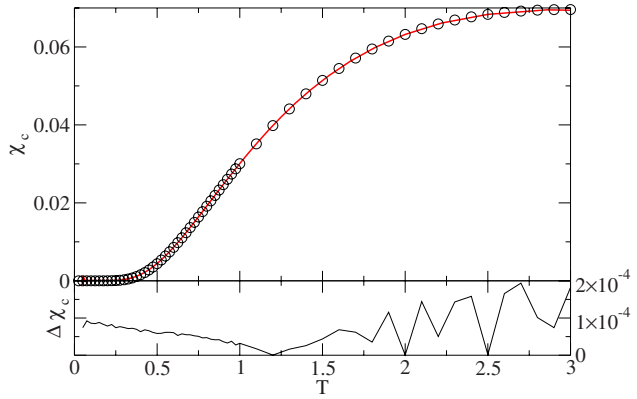

FIG. 3. (Color online) Same as Fig. 1 for the charge susceptibility χ_c.

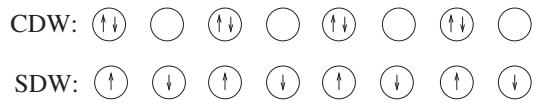

FIG. 4. The two ground states in the strong-coupling limit $U,V \gg t$. The state in the first line is a CDW state where every second site is doubly occupied, whereas the state in the second line is a state with every site singly occupied. Virtual hopping processes induce a quasi-long-range SDW order for this state.

A. Strong coupling

In the strong-coupling limit, $U,V \gg t$, the ground state energy can be systematically expanded in terms of the hopping parameter t. In lowest order, the hopping can be completely neglected. Then, depending on the ratio U/V, two different ground states are possible. These states are depicted in Fig. 4. The energy of the CDW state is then given by $E^0_{CDW} = LU/4 - LV$, with L being the number of lattice sites. The SDW state has energy $E^0_{SDW} = -LU/4$. The two energies as a function of U,V cross at $U=2V$, resulting in a first order phase transition. As usual, in second order in t, virtual hopping processes lead to an effective antiferromagnetic coupling of Heisenberg type for the spins in the SDW state with coupling constant $J = 2t^2/(U-V)$.[1,3] This state therefore has a charge gap but no spin gap and algebraically decaying spin correlation functions. The CDW state, on the other hand, has a charge and a spin gap. Excitations for the CDW and SDW states, ignoring hopping processes, are shown in Fig. 5. In lowest order perturbation theory, the energies of the excited states depicted in Fig. 5 are given by $E^1_{CDW} = E^0_{CDW} - U/2 + 2V$, $E^2_{CDW} = E^0_{CDW} - U + 3V$ for the excited CDW states and $E^1_{SDW} = E^0_{SDW} + U/2$, $E^2_{SDW} = E^0_{SDW} + U - V$ for the excited SDW states. Excitation (1) in the CDW state is a charge excitation, whereas the breaking of a double occupancy—excitation (2)—is a spin excitation. If we separate the two single spins in this excited state, we obtain an excitation energy $E^0_{CDW} + 2(-U/2 + 2V)$, i.e., each single spin contributes $-U/2 + 2V$.

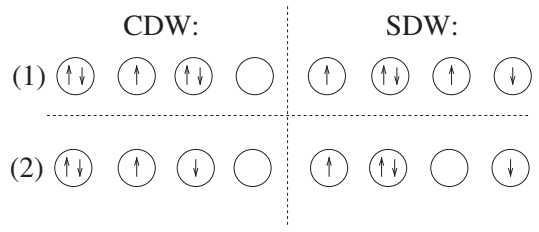

FIG. 5. Left column: (1) CDW state with one particle added and (2) CDW state with one double occupancy broken. Right column: (1) SDW state with one particle added and (2) SDW state with one double occupancy.

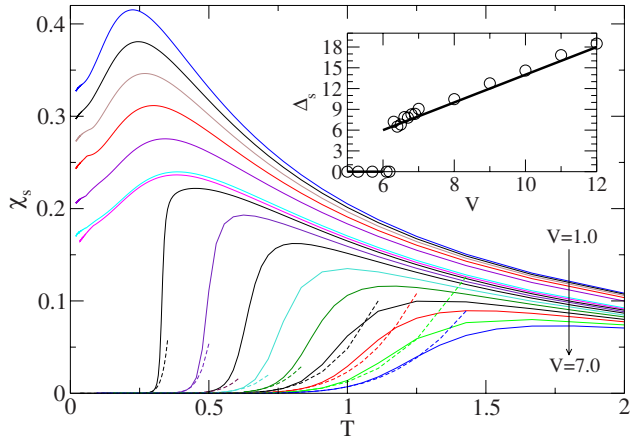

FIG. 6. (Color online) Magnetic susceptibilities (solid lines) for $U=12$ and $V=1.0,2.0,\ldots,6.0,6.1,6.2,\ldots,7.0$ as a function of temperature T. The dashed lines are fits according to Eq. (3). The inset shows the spin gap Δ_s extracted from those fits (circles) as a function of V. The solid lines in the inset denote the theoretical result in the strong-coupling limit.

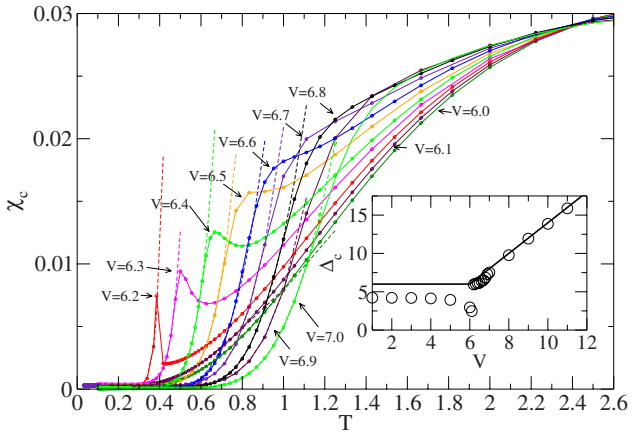

FIG. 7. (Color online) Charge susceptibilities (circles) for $U=12$ and $V=6.0,6.1,\ldots,7.0$ as a function of temperature T. The lines are a guide to the eye. The dashed lines are fits according to Eq. (3). The inset shows the charge gap Δ_c extracted from those fits (circles) as a function of V. The solid lines in the inset denote the theoretical result in the strong-coupling limit.

In thermodynamic data, the activated behavior will be characterized by the energy of a single excitation irrespective of whether these excitations appear in pairs or not. In the strong-coupling limit, it follows that at the transition line charge and spin gap as obtained from thermodynamic data are expected to be equal $\Delta_s=\Delta_c=U/2$ and that both gaps increase linearly $\sim 2V$ away from the transition line. In the SDW phase, excitation (1) is also a charge excitation and has a lower energy than excitation (2). The charge gap in the SDW phase is therefore given by $\Delta_c=U/2$ and is independent of V.

In Fig. 6, TMRG results for the spin susceptibility χ_s and the spin gap Δ_s at $U=12$ are shown. If a gap Δ exists, the dispersion of the elementary excitations is given by $\epsilon(k) \sim \Delta + k^2/(2m)$ with some effective mass m. It is then easy to see that the corresponding susceptibility will show activated behavior,

$$\chi(T) \sim \frac{\exp(-\Delta/T)}{\sqrt{T}}, \tag{3}$$

at temperatures $T \ll \Delta$. Using this function to fit the numerical data, we are able to extract the spin gap Δ_s. As shown in the inset of Fig. 6, the behavior of Δ_s as a function of V at $U=12$ is already reasonably well described by the strong-coupling limit, i.e., there is no spin gap up to $V \approx U/2$, and then Δ_s jumps to approximately $U/2$ and then increases linearly with slope 2.

Similarly, we show TMRG results for the charge susceptibility χ_c and the charge gap Δ_c at $U=12$ in Fig. 7. The results obtained for the charge gap Δ_c are also already close to the strong-coupling limit, although the gap is a bit smaller than $U/2$ in the SDW phase and it shows some V dependence when the transition point is approached.

Another quantity which allows us to detect the phase transition and to determine its order is the double occupancy

$$d = \langle n_{j,\uparrow} n_{j,\downarrow} \rangle. \tag{4}$$

In the strong-coupling limit at zero temperature, $d=0$ in the SDW state and $d=1/2$ in the CDW state. In Fig. 8, we show d for $U=12$ and various V. In the extrapolated data for zero temperature, some corrections to the strong-coupling limit are visible. d is already nonzero in the SDW phase and increases slightly with V. However, a jump in d at $V \approx 6.18$ is obvious. In the CDW phase d continues to increase with V and approaches $1/2$ in the large V limit.

The specific heat shown in Fig. 9 has two maxima for $U=12$ and $V=0$. The lower- and higher-temperature maxima are due to spin and (gapped) charge excitations, respectively.[17] At low temperatures, only the gapless spin excitations do therefore contribute, and conformal field theory predicts

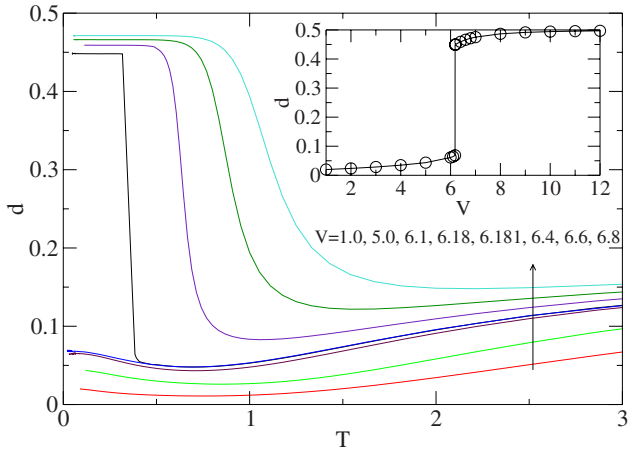

FIG. 8. (Color online) Double occupancy as a function of temperature for $U=12$ and different V. Inset: Extrapolated values of the double occupancy at zero temperature as a function of V.

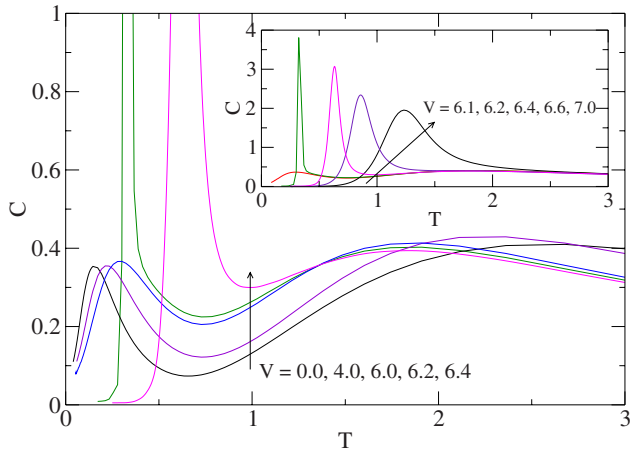

FIG. 9. (Color online) Specific heat as a function of temperature for $U=12$ and different V. Inset: A sharp peak forms just above phase transition.

$$C = \frac{\pi}{3v_s} T. \tag{5}$$

With increasing V, the spin velocity v_s increases leading to a decreasing slope and to a shift of the lower-temperature maximum to higher temperatures. At the same time, the charge gap decreases leading to a shift of the higher-temperature maximum to lower temperatures. The behavior changes drastically above the phase transition $V > V_c \approx 6.18$, because in the CDW phase, the spin excitations are now also gapped and the specific heat shows activated behavior $C \sim e^{-\Delta/T}$ with $\Delta = \min(\Delta_s, \Delta_c)$. The emergence of a sharp peak for $V \gtrsim V_c$ can be understood as follows: Because $\int_0^\infty C(T)dT = -e_0$, with e_o being the ground state energy, the area under the curve will be nearly unchanged when going from a value just below the phase transition, say, $V=6.1$, to a value just above the transition, say, $V=6.2$. In addition, also the high-temperature behavior will be almost unaffected by this small change in V. Hence, the weight suppressed by the gap at low temperatures will show up in a sharp peak just above the gap. This is shown in the inset of Fig. 9 and constitutes one possibility to detect the first order transition easily from thermodynamic data.

B. Tricritical point

From the discussion in the Introduction, it is clear that the first order transition line must end at some point (U_t, V_t) because the phase transitions at weaker couplings are expected to be continuous. We found that a good criterion to determine this endpoint with the TMRG method is to study the double occupancy d [Eq. (4)]. As shown for the case $U=12$ in Fig. 8, d as a function of T shows a dramatically different behavior depending on weather we choose a V such that we are in the SDW phase or a V such that we are in the CDW phase. d at a fixed U extrapolated to zero temperature therefore shows a jump Δ_d as a function of V if the phase transition is of first order. Reducing the on-site repulsion U, we expect this jump to become smaller and smaller until it disappears at U_t. For $U=7.0$, we can still detect a finite jump ~ 0.17 at $V \approx 3.65$ [see Fig. 10(c)], whereas d as a function of V seems to be continuous for $U=6$ [see Fig. 10(b)]. To determine the point (U_t, V_t) more accurately, we have plotted the jump Δ_d as a function of U in Fig. 10(d). We can fit these data very well by a power law which leads us to the estimate $U_t = 6.7 \pm 0.2$. Because the value for $U=7$ is least reliable, we also did fits where this point was excluded. Similarly, we tried fits where the data points for large U were excluded. The results of the various fits lead to the error estimate above. For each possible value of U_t, we can find V_t with high accuracy. For the values of U_t estimated above, we have $V_t = 3.5 \pm 0.1$. Here, the uncertainty in V_t is not an error estimate but rather means that $V_t \approx 3.4$ for $U_t = 6.5$ and $V_t \approx 3.6$ for $U_t = 6.9$.

C. Weak coupling

The phase diagram in the weak-coupling limit is more complicated than in the strong-coupling limit. Instead of a first order, we expect different continuous phase transitions here. Theoretically, the weak-coupling limit can be investigated by bosonization with the coupling constants of the operators in the effective Hamiltonian being determined in first order in the interaction parameters. This method is also often termed g-ology.[5] As usual in one dimension, the charge and the spin sectors completely separate in the low-energy effective bosonic theory due to the linearization of the excitation spectrum. In the charge sector at half filling, umklapp scattering leads to a relevant interaction term in the bosonic Hamiltonian which creates a charge gap. In the spin sector, on the other hand, the leading interaction term corresponding to backward scattering is only marginal. The amplitudes of both terms in the weak-coupling limit are proportional to $U-2V$.[4] The system therefore has always a charge gap except at $U=2V$, where the amplitude of the umklapp scattering term vanishes. The charge gap at fixed U near the phase transition behaves as

$$\Delta_c \sim |V - V_c|^\alpha, \tag{6}$$

with $\alpha > 0$ being an interaction dependent critical exponent and $V_c \approx U/2$ at weak coupling. This means that the transition in the charge sector is of second order. In the spin sector at weak coupling, the backward scattering term is marginally irrelevant if $U > 2V$ so that the spin excitations are gapless. For $U < 2V$, this term becomes marginally relevant and a spin gap Δ_s appears. However, this gap only opens up exponentially slow, i.e., for a fixed U and $V \gtrsim V_c$, we expect

$$\Delta_s \sim \sqrt{V - V_c}\, \exp\{-\text{const}/(V - V_c)\}, \tag{7}$$

with $V_c \approx U/2$ at weak coupling.[18] The phase transition in the spin sector is therefore of Kosterlitz-Thouless (KT) type.

As Nakamura[6] first noted, there is no symmetry which fixes the amplitude of the umklapp and backward scattering terms to be the same. So although these amplitudes are identical to first order in the interaction parameters, one would expect, in general, that they start to differ once higher order corrections are taken into account. In this case, an additional phase between the SDW and CDW phases would occur. As

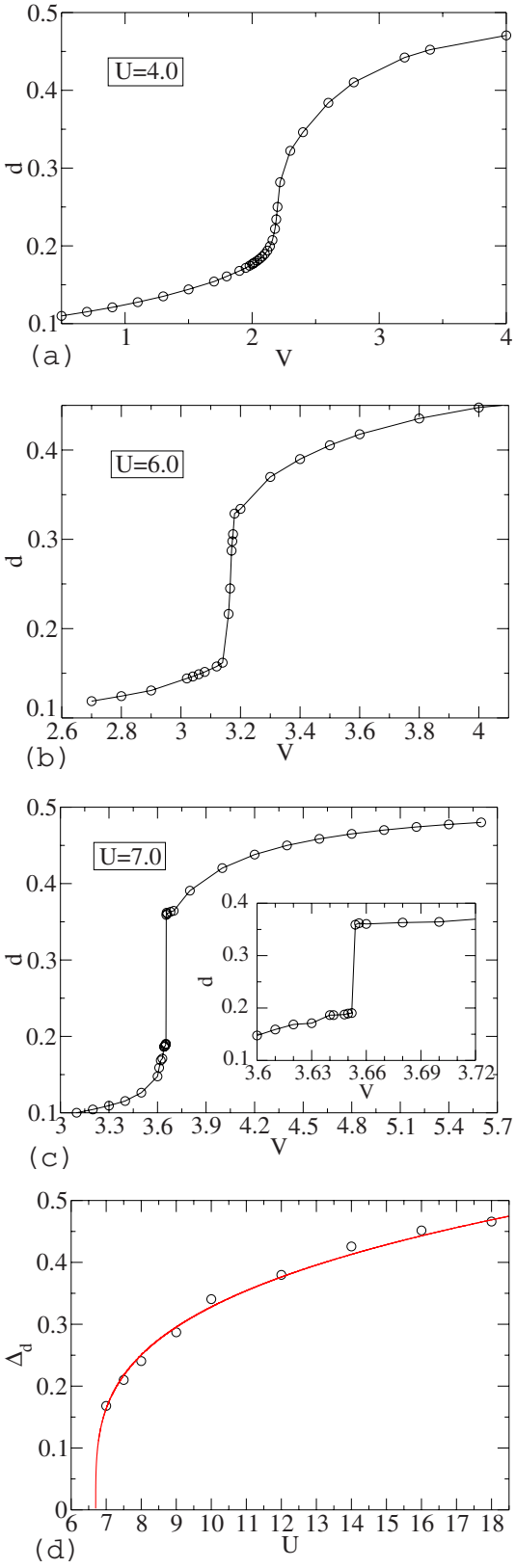

FIG. 10. (Color online) Extrapolated values of the double occupancy d at zero temperature as a function of V for different U. The inset of (c) shows a zoom of the region where d jumps. (d) Extrapolated TMRG data (circles) for the jump Δ_d in the double occupancy at the phase transition at zero temperature as a function of U. The line is a fit $\Delta_d = 0.232(U-6.7)^{0.29}$.

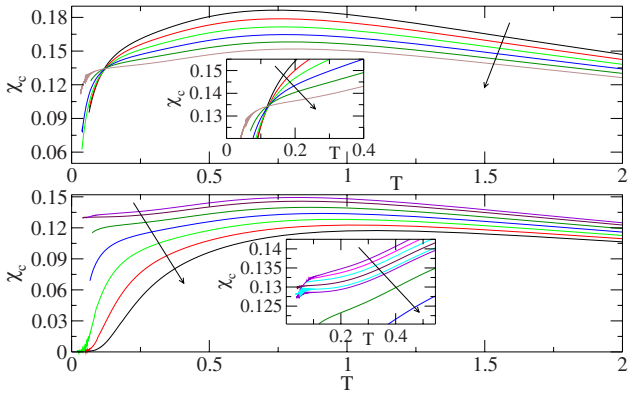

FIG. 11. (Color online) Charge susceptibility χ_c for $U=2$. Upper panel: χ_c for $V=0.5, 0.6, \ldots, 1.0$ (in arrow direction). The inset shows a zoom of the region around the crossing point at $T^* \approx 0.12$. Lower panel: χ_c for $V=1.04, 1.1, 1.2, \ldots, 1.6$ (main, in arrow direction) and $V=1.04, 1.06, 1.08, 1.1, 1.12, 1.13, 1.2, 1.3$ (inset, in arrow direction).

already outlined in the Introduction, different methods have given strong evidence that an additional phase with BOW order does indeed exist, although some controversy about the extent of this additional phase remains.[4,6–12]

In the following, we will first develop a criterion which allows us to determine the second order line where the charge gap closes with high precision from thermodynamic data. Next, we will consider the KT-type transition where the spin gap opens. Finally, we will provide some direct evidence that the phase has long-range BOW order at zero temperature and does not extend beyond the tricritical point.

To determine the line in the U,V-phase diagram where the charge gap closes, we consider the charge susceptibility χ_c. If a charge gap Δ_c exists, χ_c at temperatures $T \ll \Delta_c$ is described by Eq. (3). In the low-temperature regime, χ_c therefore will be larger the smaller the charge gap is. According to Eq. (6), we therefore expect the following behavior of $\chi_c(T_0, V)$ at fixed U and fixed low temperature T_0: If $V < V_c$, then $\chi_c(T_0, V)$, increases with increasing V, whereas $\chi_c(T_0, V)$ decreases with increasing V if $V > V_c$.

For high temperatures, $T_0 \gg 1$, on the other hand, $\chi_c(T_0, V)$ will always decrease with increasing V as can be easily seen from a high-temperature expansion. Up to second order in $1/T$, we find

$$\chi_c(T \gg 1) = \frac{1}{2T}\left[1 - \frac{1}{2T}\left(\frac{U}{2} + V\right)\right]. \tag{8}$$

For $V < V_c$, we therefore have the situation that $\partial\chi_c/\partial V > 0$ for $T \ll 1$ and $\partial\chi_c/\partial V < 0$ for $T \gg 1$. The compressibility curves for different $V < V_c$ at fixed U therefore have to cross at least at one point. For $V > V_c$, on the other hand, we have $\partial\chi_c/\partial V < 0$ for high as well as for low temperatures so that no crossing is expected. The different behavior of the compressibility curves for $V > V_c$ and $V < V_c$ is a very efficient criterion to determine V_c as is shown in Figs. 11 and 12 for the cases $U=2$ and $U=4$, respectively. From Fig. 11, lower panel, we see that the first curve crossing the ones for larger

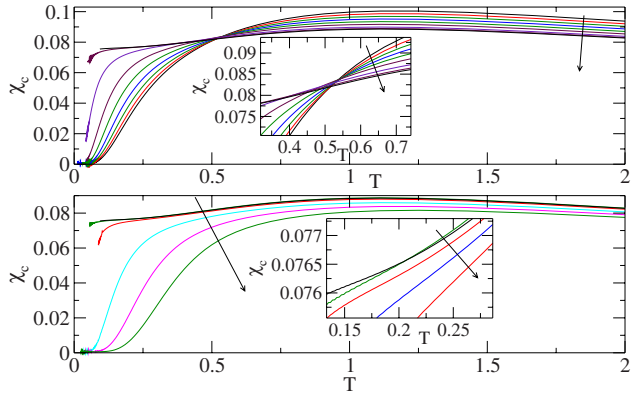

FIG. 12. (Color online) Charge susceptibility χ_c for $U=4$. Upper panel: χ_c for $V=1.5,1.6,\ldots,2.1,2.15,2.17$ (in arrow direction). The inset shows a zoom of the region around the crossing point at $T^* \approx 0.54$. Lower panel: χ_c for $V=2.16,2.17,2.2,2.3,2.4,2.5$ (main, in arrow direction) and $V=2.16,2.17,2.18,2.19,2.2$ (inset, in arrow direction).

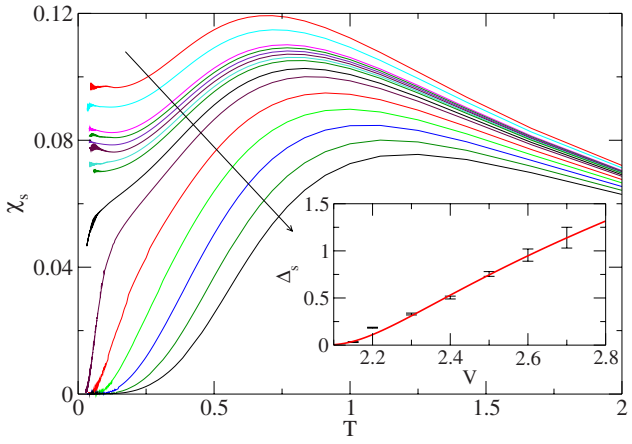

FIG. 13. (Color online) Spin susceptibility at $U=4$ for different $V=1.8,1.9,2.0,2.02,\ldots,2.1,2.15,2.2,2.3,\ldots,2.7$. Inset: Spin gap Δ_s at $U=4$ as a function of V. The gap is well fitted by $\Delta_s \sim 2.52\sqrt{V-2.02}\exp[-0.41/(V-2.02)]$.

V is the one for $V=1.04$. We therefore find $V_c=1.05\pm0.01$ for $U=2$. In principle, the critical point can be determined with this method even more accurately. Similarly for $U=4$, the inset of the lower panel of Fig. 12 shows that the first curve crossing is $V=2.16$, which leads to the estimate $V_c=2.165\pm0.005$ in this case. Both critical values are in good agreement with the most recent zero-temperature DMRG calculation.[11] Another interesting point is that in both cases, the curves for $V<V_c$ do not only cross but do so at one well defined point. That is, there is a well defined temperature T^* where $\partial\chi_c/\partial V \approx 0$ for all V. Similar well defined crossing points have also been observed in other systems and other thermodynamic quantities, as for example, the specific heat.[19,20]

For the spin susceptibility χ_s, there is only a spin gap above the KT transition. For $V>V_c^{KT}$, the temperature dependence of the spin susceptibility is then again given by Eq. (3). $\partial\chi_s/\partial V<0$ for all temperatures so that the curves do not cross. The same is true for $V<V_c^{KT}$: In the low-temperature limit, the spin sector is then described by conformal field theory and

$$\chi_s(T=0)=\frac{1}{2\pi v_s}. \tag{9}$$

The spin velocity v_s increases with increasing interaction strength so that again $\partial\chi_s/\partial V<0$ for all temperatures. Therefore, no qualitative change happens at the transition line. In principle, one can try to use the fact that there is universal scaling of certain ratios of thermodynamic quantities in the conformal regime. The entropy is given by Eq. (5) so that

$$\lim_{T\to 0}\frac{S}{T\chi_s}\equiv\frac{2\pi^2}{3} \tag{10}$$

is universal in the regime with gapless spin excitations. However, these formulas are only valid at temperatures $T \ll \Delta_c$. Because the spin gap opens close to the point where the charge gap vanishes, this criterion turns out to be useless for our numerical calculations. We therefore have to determine the KT line by directly extracting the gap from the susceptibility curves. As an example, we consider again the case $U=4$ (see Fig. 13). For small V, the behavior is qualitatively consistent with Eq. (9), whereas for large V, a spin gap is clearly visible. Fitting the low-temperature part of the curves where a gap is present using Eq. (3), we can extract Δ_s as a function of V as shown in the inset of Fig. 13. Here, the error bars are obtained by varying the fit region. Another fit according to Eq. (7) then yields $V_c^{KT}\approx 2.02\pm0.06$, where the error estimate stems again from a variation of the fit region. Within the estimated errors, we therefore obtain strong evidence that $V_c \neq V_c^{KT}$ for $U=4$, i.e., that we have two separate phase transitions. Following this procedure to determine the second order and the KT transition lines for other values of U, we obtain the phase diagram discussed in the next section.

D. Phase diagram

Our phase diagram, shown in Fig. 14, is very similar to the one obtained in the most recent zero-temperature DMRG study.[11] There is a first order transition line for (U,V) values above the tricritical point (U_t,V_t) separating the SDW and CDW phases. Below the tricritical point, we have a KT-type transition line where the spin gap opens and a second order phase transition line where the charge gap disappears. The nature of the so-called BOW phase enclosed by the two transition lines is discussed in more detail in the next section. There is some quantitative difference between our study and Zhang's DMRG study[11] in the location of the tricritical point though. We find $U_t=6.7\pm0.2$, $V_t=3.5\pm0.1$, whereas he found $U_t\approx 7.2$, $V_t\approx 3.746$. Both values are considerably larger than the ones found in QMC calculations, $U_t=4.7\pm0.1$, $V_t=2.51\pm0.04$ in Ref. 7, and $U_t\in[5,5.5]$ in Ref. 8. We also note that our phase diagram disagrees with that obtained in an earlier DMRG calculation[10] where the BOW phase was restricted to the first order phase transition line (SDW-CDW)

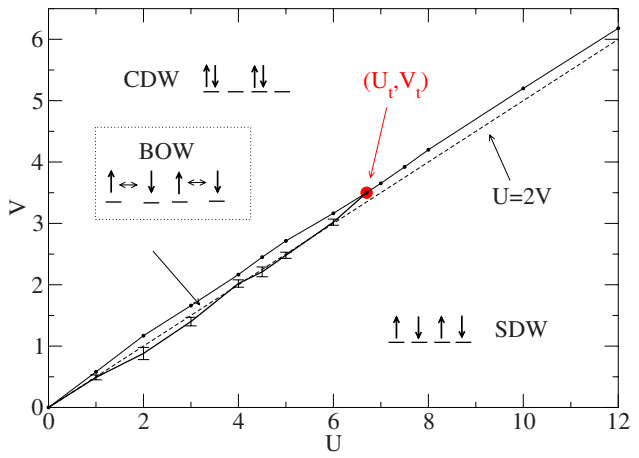

FIG. 14. (Color online) Phase diagram as obtained by TMRG. The dashed line denotes $U=2\ V$. The upper line describes the phase boundary of the CDW phase. The related error is always smaller than the symbol size. The error of the KT phase transition (lower line) is shown.

extending from above the tricritical point estimated to be at $U_t=3.7\pm0.2$ up to $U\approx 8$.

E. Long-range bond-order wave order and extent of the bond-order wave phase

From the phase diagram, Fig. 14, we see that the spin gap opens starting from the SDW phase and only after that the transition into the CDW phase occurs. From field theoretical considerations, it is then expected that the phase enclosed by these two transition lines is a Mott state with some dimerization, also called a bond-order wave (BOW) state. Because such a dimerization does not break any continuous symmetry, true long-range order at zero temperature will occur even in one dimension. This means that for the correlation function

$$F(r)=(-1)^r(\langle A_0A_r\rangle-\langle A_r\rangle^2), \tag{11}$$

with $A_r=S^z_rS^z_{r+1}$ or $A_r=\Sigma_\sigma(c^\dagger_{r,\sigma}c_{r+1,\sigma}+\text{H.c.})$, we have $\lim_{r\to\infty}F(r)=\text{const}\neq 0$. With the TMRG algorithm, there are different possibilities to detect this order. First, next-leading eigenvalues of the QTM allow it to calculate correlation lengths easily. In an asymptotic expansion of a two-point correlation function with operator O_r, we obtain

$$\langle O_1O_r\rangle-\langle O_1\rangle\langle O_r\rangle=\sum_\alpha M_\alpha e^{-r/\xi_\alpha}e^{ik_\alpha r}, \tag{12}$$

with correlation lengths ξ_α and wave vectors k_α given by

$$\xi_\alpha^{-1}=\ln\left|\frac{\Lambda_0}{\Lambda_\alpha}\right|,\quad k_\alpha=\arg\left(\frac{\Lambda_0}{\Lambda_\alpha}\right), \tag{13}$$

where Λ_0 is the largest eigenvalue of the QTM and Λ_α another eigenvalue. A correlation length obtained according to Eq. (13) will show up in the asymptotic expansion (12) if the corresponding matrix element M_α, which can also be calculated with the TMRG algorithm,[15,21] is nonzero. In the long-distance limit, the behavior of the correlation function will be determined by the largest correlation length ξ with nonzero matrix element.

If the correlation function decays algebraically, this correlation length will diverge like $\xi\sim 1/T$. If, on the other hand, the correlation function decays exponentially even at zero temperature, then ξ stays finite. Finally, for a correlation function showing true long-range order at zero temperature, the correlation length will diverge like

$$\xi\sim\frac{\exp(\Delta/T)}{\sqrt{T}}, \tag{14}$$

where Δ is the gap for the corresponding excitations.

In Fig. 15(a), we show, as an example, the leading SDW, CDW, and BOW correlation lengths for $U=6$ and $V=3.16$. Here, the leading SDW and CDW correlation lengths stay finite, whereas the BOW correlation length diverges faster than $1/T$, indicating long-range BOW order at zero temperature.

Another possibility to detect the BOW order with the TMRG algorithm is to calculate static susceptibilities

$$\chi_{OO}(q)=\sum_r e^{iqr}\int_0^\beta d\tau\langle O_0(0)O_r(\tau)\rangle \tag{15}$$

again for some operator O_r. For true long-range order, the corresponding $\chi(q)$ will diverge exponentially with temperature, whereas $\chi(q)$ will go to a constant (zero if the operator is conserved) for short-range order. The situation is, however, complicated if the correlation function shows quasi-long-range order, i.e., decays algebraically. Here, we want to consider the case that only one sort of excitations is gapless, say, the spin excitations. From conformal field theory, it is known that the corresponding algebraically decaying correlation function in the long-distance limit $r\gg 1$ will behave as

$$\langle O_0(0)O_r(\tau)\rangle\sim\left(\frac{2\pi T}{v}\right)^{2x}\exp\left[\frac{-2\pi Tx}{v}r\right]\times\exp[-ikr]\exp[2\pi Ti(d^+-d^-)\tau]. \tag{16}$$

Here, v is the velocity of the elementary excitations, $x=d^+ +d^-$ the scaling dimension, $d^\pm$ the conformal weights, and k the characteristic wave vector. The τ integral for the static susceptibility $\chi_{OO}(k)$ can then be calculated explicitly and is given by

$$\int_0^\beta d\tau\exp[2\pi Ti(d^+-d^-)\tau]=\frac{e^{2\pi i(d^+-d^-)}-1}{2\pi iT(d^+-d^-)}. \tag{17}$$

If the conformal spin $s=d^+-d^-$ is a nonzero integer—this is the case for any type of particle-hole excitation—the integral is zero and this part of the correlation function does not contribute. If, on the other hand, $s=0$, then there is no time dependence in Eq. (16) and integral (17) yields just $1/T$. The static susceptibility in the case of zero conformal spin will therefore scale as $\chi_{OO}(k)\sim T^{2x-2}$. In particular, for the alternating part of the longitudinal spin-spin correlation function, we have $d^+=d^-=1/4$ leading to $\chi_{S^zS^z}(\pi)\sim 1/T$. Note, however, that for $x>1$, the long-distance asymptotics is no

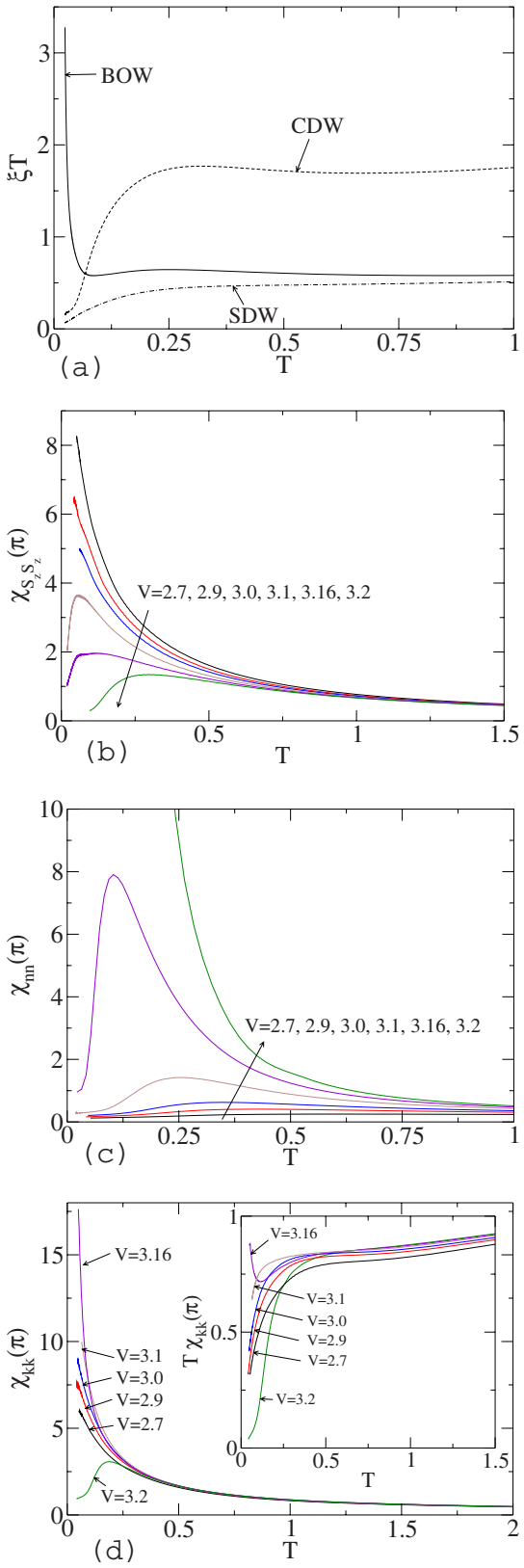

FIG. 15. (Color online) (a) Leading SDW, CDW, and BOW correlation lengths plotted as ξT for $U=6$ and $V=3.16$. [(b)–(d)] Alternating static susceptibilities for the longitudinal spin, the density, and the kinetic energy $k=\Sigma_\sigma(c^\dagger_{r,\sigma}c_{r+1,\sigma}+\text{H.c.})$ for $U=6$ and different V, respectively.

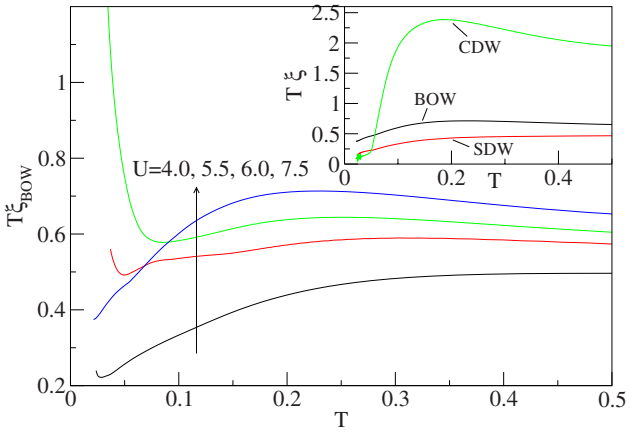

FIG. 16. (Color online) Leading BOW correlation lengths for $(U,V)=(4.0,2.14),(5.5,2.9),(6.0,3.19),(7.5,3.9)$. The inset shows the leading BOW, SDW, and CDW correlation lengths for $(U,V)=(7.5,3.9)$.

longer sufficient to discuss the behavior for $T\to 0$. In this case, $\chi_{OO}(k)\to$const for a nonconserved operator, in general, as in the case of exponentially decaying correlation functions discussed above.

In Figs. 15(b)–15(d), we show for $U=6$ and different V the alternating static susceptibilities for the longitudinal spin, the density, and the kinetic energy, respectively. From Fig. 15(b), we conclude that a spin gap develops for $V\gtrsim 3.1$. However, for $V=3.1$ and $V=3.16$, there is still no long-range charge order [see Fig. 15(c)], i.e., an intermediate phase does exist. In Fig. 15(d), we see that at least for $V=3.16$, this phase has long-range BOW order which is consistent with the correlation lengths shown in Fig. 15(a). Fitting the BOW correlation length using Eq. (14), we extract a rather small dimer gap $\Delta\sim 0.08$. For fixed U, the dimer gap is expected to decrease with decreasing V so that possible long-range bond order is detected most easily close to the transition into the CDW phase. In Fig. 16, the leading BOW correlation lengths for several U,V values just below this transition line are shown. For $(U,V)=(4.0,2.14)$, (5.5, 2.9), and (6.0, 3.19), the correlation lengths diverge exponentially, and we obtain the dimer gaps $\Delta\approx 0.01$, 0.03, and 0.08, respectively. As expected, Δ decreases with decreasing U, making it difficult to show the exponential divergence of the BOW correlation length for $U<4$ because temperatures below $T\sim 10^{-2}$ are not easily accessible by the TMRG method. Nevertheless, it is clear that the whole phase enclosed by the two transition lines shown in Fig. 14 must have long-range BOW order. For $(U,V)=(7.5,3.9)$, on the other hand, we would expect $\Delta\gtrsim 0.1$ if BOW order does exist as found in Ref. 8 so that an exponential divergence should already become obvious at $T\sim 0.1$. However, down to $T\approx 0.02$, we see no indication of such a behavior; instead, the BOW correlation length seems to diverge exactly as $1/T$, indicating that we are in the SDW phase. This is supported by the data in the inset of Fig. 16 showing that the leading SDW correlation length also diverges like $1/T$, whereas the CDW correlation length stays finite for $T\to 0$. Interestingly, the BOW correlation length is larger than the SDW correlation length. We also confirmed

that for $(U,V)=(7.5,3.92)$, we are already in the CDW phase. We therefore conclude that for $U=7.5$, no BOW phase exists. Instead, a direct first order transition from the SDW to the CDW phase occurs.

IV. SUMMARY AND CONCLUSIONS

We studied the thermodynamics of the half-filled one-dimensional extended Hubbard model using a TMRG algorithm. The focus was put on identifying the various phase transitions by considering thermodynamic quantities which are usually easy to measure such as the uniform magnetic susceptibility χ_s or the isothermal compressibility χ_c. For strong coupling, we calculated the charge gap in the SDW as well as charge and spin gap in the CDW phase in lowest order perturbation theory. The theoretical results were confirmed by TMRG calculations of χ_s and χ_c. In the weak-coupling regime, where the phase transitions are continuous, we showed that χ_c curves for a fixed U and different V as a function of temperature cross in one well defined point if measured in the SDW or BOW phase. In the CDW phase, on the other hand, no crossing occurs. We used this criterion to determine the boundary of the CDW phase with high accuracy. The KT transition line, on the other hand, where the spin gap starts to open exponentially slowly is very difficult to determine from thermodynamic data. Universal scaling relations obtained from conformal field theory for the magnetic susceptibility and the specific heat in the SDW phase turned out to be useless for this purpose. These scaling relations are only valid at temperatures $T \ll \Delta_c$ which are not accessible by TMRG, because the charge gap Δ_c is already very small near the KT transition. We could, however, show that extracting the spin gap from the magnetic susceptibility where it is large enough and fitting it to a field theory formula does allow us to determine the transition line reasonably well. In particular, the results clearly confirm that the two transition lines do not coincide and that an intermediate phase exists. By studying correlation lengths and static susceptibilities, we confirmed that this additional phase has long-range bond order. We were also able to determine the tricritical point accurately and found $U_t=6.7\pm0.2$, $V_t=3.5\pm0.1$. Furthermore, we showed that above this point, long-range bond order does not exist. Instead, we find that BOW correlations can be dominant in this regime while still decaying algebraically at zero temperature. The resulting phase diagram is in good quantitative agreement with the most recent zero-temperature DMRG study.[11] However, it does not agree with the phase diagram found in Ref. 8 with the BOW phase existing even above the tricritical point.

ACKNOWLEDGMENTS

The authors acknowledge helpful discussions with E. Jeckelmann and S. Nishimoto. This work has been supported by the DFG Schwerpunkt SP1073 and Graduiertenkolleg GK1052 (S.G. and A.K.).

[1] J. E. Hirsch, Phys. Rev. Lett. **53**, 2327 (1984).
[2] R. A. Bari, Phys. Rev. B **3**, 2662 (1971).
[3] P. G. J. van Dongen, Phys. Rev. B **49**, 7904 (1994).
[4] M. Nakamura, Phys. Rev. B **61**, 16377 (2000).
[5] J. Sólyom, Adv. Phys. **28**, 201 (1979).
[6] M. Nakamura, J. Phys. Soc. Jpn. **68**, 3123 (1999).
[7] P. Sengupta, A. W. Sandvik, and D. K. Campbell, Phys. Rev. B **65**, 155113 (2002).
[8] A. W. Sandvik, L. Balents, and D. K. Campbell, Phys. Rev. Lett. **92**, 236401 (2004).
[9] M. Tsuchiizu and A. Furusaki, Phys. Rev. Lett. **88**, 056402 (2002).
[10] E. Jeckelmann, Phys. Rev. Lett. **89**, 236401 (2002).
[11] Y. Z. Zhang, Phys. Rev. Lett. **92**, 246404 (2004).
[12] K.-M. Tam, S.-W. Tsai, and D. K. Campbell, Phys. Rev. Lett. **96**, 036408 (2006).
[13] *Density-Matrix Renormalization*, edited by I. Peschel, X. Wang, M. Kaulke, and K. Hallberg, Lecture Notes in Physics Vol. 528 (Springer, Berlin, 1999), and references therein.
[14] S. Glocke, A. Klümper, and J. Sirker, in *Density-Matrix Renormalization Group for Transfer Matrices: Static and Dynamical Properties of 1D Quantum Systems at Finite Temperature*, Lecture Notes in Physics Vol. 739 (Springer, Berlin, in press), pp. 665–677.
[15] J. Sirker and A. Klümper, Europhys. Lett. **60**, 262 (2002).
[16] G. Jüttner, A. Klümper, and J. Suzuki, Nucl. Phys. B **522**, 471 (1998).
[17] G. Jüttner, A. Klümper, and J. Suzuki, Nucl. Phys. B **487**, 650 (1997).
[18] M. Nakamura, A. Kitazawa, and K. Nomura, Phys. Rev. B **60**, 7850 (1999).
[19] D. Vollhardt, Phys. Rev. Lett. **78**, 1307 (1997).
[20] A. Kemper and A. Schadschneider, Phys. Rev. B **68**, 235102 (2003).
[21] J. Sirker and A. Klümper, Phys. Rev. B **66**, 245102 (2002).